Clim Dyn (2011) 37:933–940
DOI 10.1007/s00382-010-0874-3

Community structure and dynamics in climate networks

Anastasios A. Tsonis · Geli Wang · Kyle L. Swanson · Francisco A. Rodrigues · Luciano da Fontura Costa

Received: 15 March 2010 / Accepted: 18 June 2010 / Published online: 6 July 2010

Abstract We consider climate networks constructed from observed and model simulated fields of three climate variables and investigate their community structure. We find that for all fields the number of effective communities is rather small (four to five). We are able to trace the origin of these communities to certain dynamical properties of climate. Our results suggest that the complete complexity of the climate system condenses beyond the 'weather' time scales into a small number of low-dimensional interacting components and provide clues as to the nature of the climate subsystems underlying these components.

Keywords Networks · Teleconnection patterns · Climate variability

1 Introduction

Climate exhibits variability over a wide range of space and time scales, from 'weather' at small spatio-temporal scales to 'climate' at large scales. However, it remains an open question whether a single dynamical system dictates the complete range of variability, or whether the high-dimensional (complicated) small-scale variability collapses at larger scales into a small number of nonlinear low-dimensional systems whose interplay adequately describes variability on these larger scales. The latter viewpoint is strongly suggested by nonlinear time series analysis of numerous records in the last 25 years. Although the procedures underlying such an analysis are rather demanding and not always applied properly, convincing evidence has emerged that variability over inter-annual, decadal, and longer time scales is characterized by small correlation dimensions (Tsonis 1992; Tsonis 2001). An interpretation of small dimensionalities in climate is that they represent the dynamics of subsystems, e.g. El Niño, which appear at specific space and time scales (Tsonis and Elsner 1989; Lorenz 1991). Up to now, however, the relevant climate subsystems and the variables defining their state space have not been adequately identified, making extensions to physics and dynamics impossible. Here we employ a newly developed approach, which not only confirms that indeed the number of subsystems is small but also identifies the geographical basis and physical mechanisms underlying these subsystems.

A network is defined by a set of nodes and their links, where any pair of nodes is connected according to some rule. The topology of the network can reveal important and novel features of the system it represents (Albert and Barabasi 2002; Strogatz 2001; da F. Costa et al. 2007). One such feature is communities (Newman and Girvan 2004). Communities represent groups of densely connected nodes with only a few connections between groups. It has been conjectured that each community represents a subsystem, which operates relatively independent of the other communities (Arenas et al. 2006). Thus, identification of these communities can offer useful insights about dynamics. In addition, communities can be associated to network

A. A. Tsonis (✉) · K. L. Swanson
Department of Mathematical Sciences, Atmospheric Sciences Group, University of Wisconsin-Milwaukee, Milwaukee, WI 53201, USA
e-mail: aatsonis@uwm.edu

G. Wang
LAGEO, Institute of Atmospheric Physics, Chinese Academy of Sciences, Beijing, China

F. A. Rodrigues · L. d. F. Costa
Institute of Physics at Sao Carlos, University of Sao Paulo, P.O. Box 369, Sao Carlos, SP 13560-970, Brazil

functions such as in metabolic networks where certain groups of genes have been identified that perform specific functions (Holme et al. 2003; Guimera and Amaral 2005). Recently, network theory has been applied to climate networks with impressive results, for example, the discovery of a new dynamical mechanism for major climate shifts (Tsonis et al. 2006; Tsonis et al. 2007; Tsonis et al. 2008; Tsonis and Swanson 2008; Yamasaki et al. 2008; Gozolchiani et al. 2008; Swanson and Tsonis 2009; Elsner et al. 2009). Here we further these analyses by investigating the presence of communities (and thus of subsystems) in the climate system.

2 Methods and results

We begin by constructing the networks for the global 500 hPa height, the global sea level pressure and the global surface temperature fields using data derived from the global National Center for Environmental Prediction/National Center for Atmospheric Research (NCEP/NCAR) atmospheric reanalysis data set (Kistler et al. 2001). These data are arranged on a grid with a resolution of 10° latitude × 10° longitude. This results in 36 points in the east–west direction and 19 points in the north–south direction for a total of $n = 684$ points. These 684 points will be assumed to be the nodes of the network. For each grid point monthly values from 1950 to 2005 are available. From the monthly values, we produced anomaly values (actual value minus the climatological average for each month). Even though the leading order effect of the annual cycle is removed by producing anomaly values, some of it is still present as the amplitude of the anomalies is greater in the winter than in the summer. For this reason, in order to avoid spurious high values of correlations, only the values for December–February in each year were considered. Thus, for each grid point we have a time series of 168 anomaly values. In order to define the links between the nodes for either network, the correlation coefficient at lag zero (r) between the time series of all possible pairs of nodes [$n(n-1)/2 = 233,586$ pairs] is estimated. Note that since the values are monthly anomalies there is very little autocorrelation in the time series. A pair is considered as connected if the absolute value of their cross-correlation $|r| \geq 0.5$. This criterion is based on parametric and non-parametric significance tests. According to the t test with $N = 168$, a value of $r = 0.5$ is statistically significant above the 99% level. In addition, randomization experiments where the values of the time series of one node in a pair are scrambled and then are correlated to the unscrambled values of the time series of the other node indicate that a value of $r = 0.5$ will not arise by chance. The choice of $r = 0.5$ while it guarantees statistical significance is somewhat arbitrary. We find that while other values might affect the connectivity structure of the network, the effect of different correlation thresholds (between 0.4 and 0.6) does not affect the conclusions reached in this study. Obviously, as $|r| \to 1$ we end up with a random network and as $r \to 0$ we remain with just one fully connected community. The use of the correlation coefficient to define links in networks is not new. Correlation coefficients have been used to successfully derive the topology of gene expression networks (Farkas et al. 2003) and to study financial markets (Mantegna 1999).

A link as defined by our correlation threshold is considered an edge connecting two geographical locations (nodes). Once the edges in a network have been defined we proceed with identifying the communities. We used several methods to identify communities. The first is based on the notion of node betweenness (Girvan and Newman 2002). For any node i, node betweenness is defined as the number of shortest paths between pairs of other nodes that run through i. The algorithm extends this definition to the case of edges, defining the "edge betweenness" of an edge as the number of shortest paths between pairs of nodes that run along this edge. If a network contains communities or groups that are only loosely connected by a few intergroup edges (think of bridges connecting different sections of New York City, for example), then all shortest paths between two nodes belonging to different communities must go along one of these few edges. Thus, the edges connecting communities will have high edge betweenness. By removing these edges, the groups are separated from one another thereby revealing the underlying community structure of the network.

Figure 1 illustrates the basics behind this algoritm. The setup is adapted from Newman and Girvan (2004). We start with a 'source' node s, which is connected to six other nodes according to the simple network shown in Fig. 1. This node is assigned a distance $d_s = 0$ and a weight $w_s = 1$. Then each node i adjacent to s (i.e. nodes 1 and 3) is given a distance $d_i = d_s + 1$ and a weight $w_i = w_s$ (1,1 and 1,1, respectively). Then each node j adjacent to nodes i is given a distance $d_j = d_{\mathrm{i}} + 1$ and weight $w_j = w_i$ and so on. This procedure results in the pairs of values shown for each node. Once distances and weights have being assigned, one finds those nodes such that no shortest paths between any other node and s pass through them. Such nodes are nodes 2, 4 and 6. We call these nodes 'leaves', and denote tham as l. For each node i neighboring l we assign a score to their edge of w_i/w_l. Accordingly, the score of the edges connecting pairs 1 and 2, 3 and 4 and 5 and 6 is equal to 1. Then we start from the edge that is farther from s (edges connecting to a leaf are not considered in this step, so that will be the edge connecting nodes 3 and 5) and assign a score that is 1 plus the sum of the scores on the

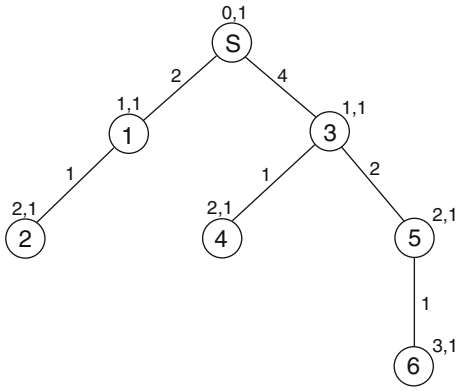

Fig. 1 An illustration of the calculation of the shortest-path betweenness. See text for details

neighboring edges immediately below it, multiplied by w_i/w_j where node j is farther from s than node i. We then move upwards repeating the process until node s is reached. This procedure will identify the edge connecting nodes s and 3 as having the highest edge betweenness. By removing it, we remain with two communities, one consisting of nodes s, 1, and 2 and another consisting of nodes 3, 4, 5, and 6. We can then continue splitting the network by removing the edge with the second highest betweenness and so on. In applications with real data, however, this approach may not work well. The reason is that it may be that there is more than one edge connecting communities. In this case, there is no guarantee that all those edges will have high betweenness. We can only be sure that at least one will have high betweenness. For this reason, the algorithm repeats the whole process for all nodes in the network (i.e. considering as the source node each node in the network at a time) and sums all the scores. This gives the total betweenness for all edges in the network. We then have to repeat this calculation for each edge removed from the network. The network is then divided into two communities by removing the edge whose removal resulted in the lowest sum, and so on.

In order to quantify the strength of a community structure we use a measure called the modularity. For a particular division into n communities we define a $n \times n$ symmetric matrix $\mathbf{e}$ whose element e_{ij} is the fraction of all connections in the network that link nodes in community i to community j. The modularity (Newman and Girvan 2004; Girvan and Newman 2002) is defined as

$$Q = \mathrm{Tr}\mathbf{e} - \left\|\mathbf{e}^2\right\|$$

where Tr is the trace of matrix $\mathbf{e}$ (the sum of the elements along the main diagonal) and $\|x\|$ indicates the sum of the elements of matrix $\boldsymbol{x}$. The modularity measures the fraction of the edges in the network that connect nodes of the same type (within-community nodes) minus the expected value of the same quantity in a network with the same community divisions but random connections between the nodes. Modularity ranges from zero (for random networks) to one (for very strong community structure). The optimum community division is found by estimating at how many communities (at what n) Q is maximum.

Figure 2 shows the division into communities of the three observed climate fields considered in this study (left panels). The top panel corresponds to the 500 hPa height network, the middle to the sea level pressure network, and the bottom to surface temperature network. The total number of communities is 47, 15, and 58, respectively. Many of these communities, however, consist of very few points in the boundaries between a small number of dominant communities (think of a country whose population is dominated by two races but also includes small groups of other races). As is evident from these panels the effective number of communities is, arguably, four in all three networks (delineated as purple, blue, green, and yellow–red areas). The modularity of the networks is 0.49, 0.56, and 0.59, respectively, indicating networks that lie between completely random and strongly communal.

Importantly, this purely mathematical approach results in divisions that have connections with actual physics and dynamics. For example, in the top left panel (500 hPa height network) we see that three of the effective four communities correspond to a latitudinal division 90°S–30°S, 30°S–30°N, and 30°N–90°N. This three-zone separation is not a trivial separation into northern hemisphere winter, southern hemisphere summer, and the rest of the world, because when we repeat the analysis with yearly averages rather than seasonal values we also see evidence of this three-zone separation. This separation is consistent with the transition from a barotropic atmosphere (where pressure depends on density only; appropriate for the tropics-subtropics) to a baroclinic atmosphere (where pressure depends on both density and temperature; appropriate for higher latitudes). Another possibility is that it reflects the well known three-zone distribution of variance of the surface pressure field. Within the third community (green area) another community (yellow–red) is embedded. This community is consistent with the presence of major atmospheric teleconnection patterns such as the Pacific North America (PNA) pattern and the North Atlantic Oscillation (NAO) (Wallace and Gutzler 1981; Barnston and Livezey 1987). We note here that NAO (which has been lately suggested of being a three-pole pattern rather than a dipole; Tsonis et al. 2008) and Arctic Oscillation (AO; Thompson and Wallace 1998) are often interpreted as manifestations of the same dynamical mode, even though in some cases more physical meaning is given to NAO (Ambaum et al. 2001). In any case, here we do not make a distinction between NAO and AO.

In the sea level pressure network, we see again the latitudinal division into three communities. Here the purple

area extends into the eastern Pacific as far as 30°N. This feature is consistent with the inter-hemispheric propagation of Rossby waves via the well documented eastern Pacific corridor (Webster and Holton 1982; Tsonis and Elsner 1996). The fourth community (yellow–red) embedded within the third community (green) is found over areas in the northern hemisphere where cyclogenesis is more frequently found. Note that PNA relates to anomalies in the forcing of extra-tropical quasi-stationary waves, the NAO arises from wave–mean flow interaction, and ENSO is known to affect extratropical cyclone variability (Eichler and Higgins 2006; Wang and Fu 2000; Held et al. 2002; Favre and Gershunov 2006; Favre and Gershunov 2009).

In the temperature network, we see a major subdivision into two communities, one covering the southern hemisphere (purple) and the other the northern hemisphere (green). This appears to be a result of the fact that the southern hemisphere is covered mostly by water (which moderates surface temperatures) whereas northern hemisphere is mostly land (where temperature variability is greater). In the northern hemisphere, we observe that embedded in the green community there is a separate community (yellow–red) over North America and North-East Asia where cold winter air outbreaks normally occur. This could be an influence of the Pacific Decadal Oscillation (PDO), which is known to affect the North American temperature anomaly structure (Mantua et al. 1997). It is interesting here that the algorithm appears to identify the moderation of temperature fluctuations in the north Atlantic and Europe due to the Gulf Stream as a different community. In the southern hemisphere embedded within the purple community, we see a separate community (blue) along the 30°S latitude. This community probably arises from the corresponding southern hemisphere storm tracks, which modify temperature fluctuations. Alternatively, it may be due to the presence of the subtropical belt. We note here that the location of some of the communities and their attributed teleconnection patterns may not be exactly the location of these patterns as delineated by empirical orthogonal function (EOF) analysis because they are different methods.

3 Sensitivity analysis

We repeated the analysis using detrended data as well as resampled data to obtain grids of equal area. The results were very similar to those in Fig. 2. The division into communities for all three networks appears consistent with known dynamics and highlights the aspects of those dynamics that dominate inter-annual to decadal climate variability. In order to further strengthen the connection between communities and teleconnection patterns we performed the following experiment. We considered the observed 500 hPa field height in the northern hemisphere and produced as before the corresponding network and found its community structure. This is our "null model" and its community structure is shown on the top of Fig. 3 where we observe three major communities (brown, green, and blue). Then, following the technique reported in Tsonis et al. (2008) and considering that EOF2 of the 500 hPa field is associated with NAO, we produced a 500 hPa height field without the NAO (by projecting the data to all but EOF2), constructed the corresponding network, and found its community structure (middle panel of Fig. 3). Similarly, by considering that EOF1 of the 500 hPa filed is associated with the PNA, we removed the PNA as well (by projecting the data to all but EOF1 and EOF2) thereby producing a field without the PNA and without NAO. We then constructed the network and found its community structure (bottom panel of Fig. 3). We observe that when we remove NAO the blue community centered in the middle North Atlantic (where NAO occurs) has largely disappeared. A community identified by the blue color is still present but has shifted eastward and away from the area where NAO occurs. The brown community includes the tropics and a spot in North America located where the PNA pattern is found. This spot remains over the same area when the NAO is removed. That this spot is associated with the community which includes the tropics is consistent with the fact that the PNA is a linear response to tropical forcing. When we remove the PNA as well, we see that the brown spot disappears. In the bottom panel there is no sign of any kind that will be consistent with the PNA or NAO. This indicates that an "alternative model" that does not contain the kind of structure in which we are interested gives results outside the range of behavior produced by the "null model". Thus, attributing communities to teleconnection patterns is rather justified.

We have carried out a number of additional network community sensitivity experiments. These experiments examined the network structure for spatio-temporal variability that is white with respect to time, and spatially correlated with a decorrelation length of 3,000 km on the sphere. A typical example of the character of the communities resulting from analyzing this type of noise is shown in Fig. 4. In general, we find the following: (1) The number of communities is roughly the area of the sphere divided by the area of a circle of radius equal to the decorrelation length, i.e. for 3,000 km there are consistently 17–20 communities. (2) The community structure is non-robust, as different realizations of the noise result in the same qualitative structure of communities (i.e. their number), but their position on the sphere is shifted. Even adding or subtracting one "year" from the synthetic data causes a leading order re-arrangement in the position of the

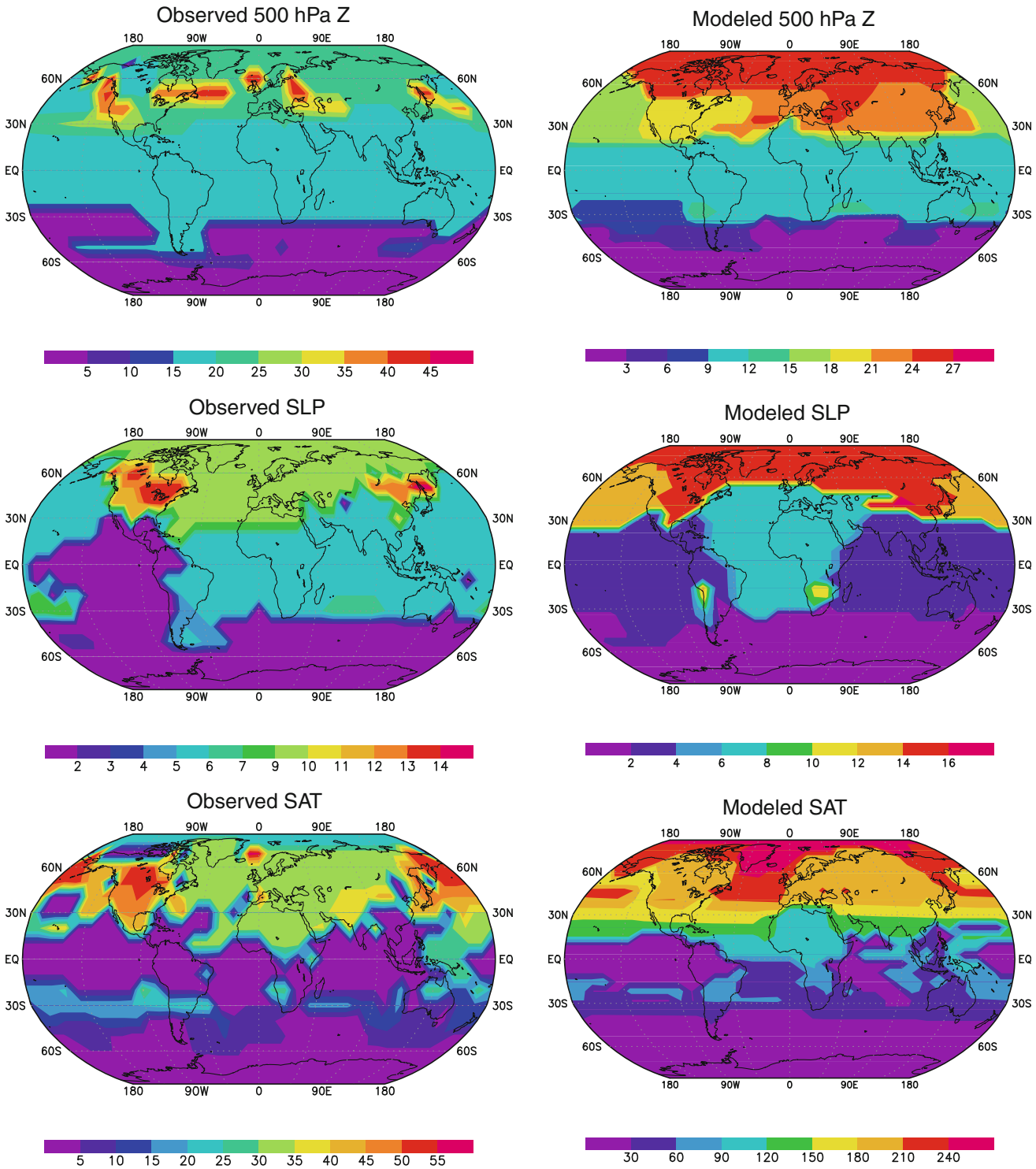

Fig. 2 Community structure in three climate networks. The networks are constructed from the 500 hPa height field (*top*), the surface pressure field (*middle*) and surface temperature field (*bottom*). The *left panels* correspond to networks constructed from observations and the *right panels* from model simulations. The number below the *shading key* indicates the total number of communities. Because the total number of communities is not necessarily the same in each network, the *color* scheme used to show the spatial delineation of the communities is not the same in each panel. This means that the same community may be represented by different *color* in the observations and in the model. The reverse may also be possible: the same *color* may not represent the same community. What we should compare in this figure is the spatial distribution and structure of communities in observations and model (see text for more details)

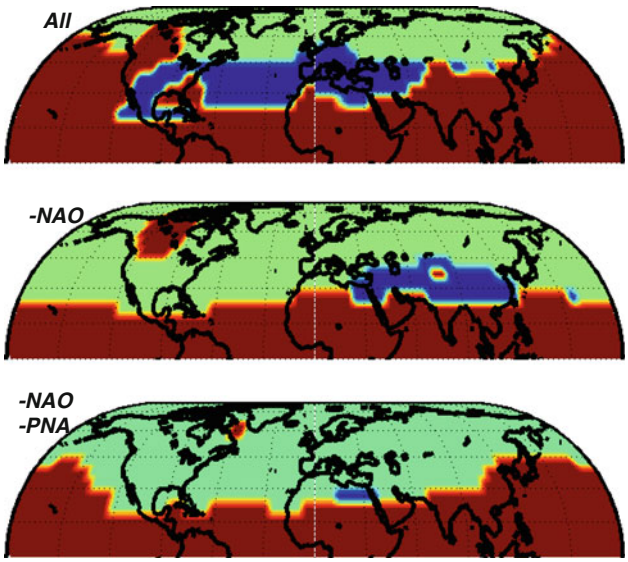

Fig. 3 Community structure in the network for the observed 500 hPa height field in the Northern hemisphere (*top*) as well as in the networks of synthetic 500 hPa height fields without the NAO (*middle panel*) and without the NAO and PNA (*bottom panel*) (see text for details)

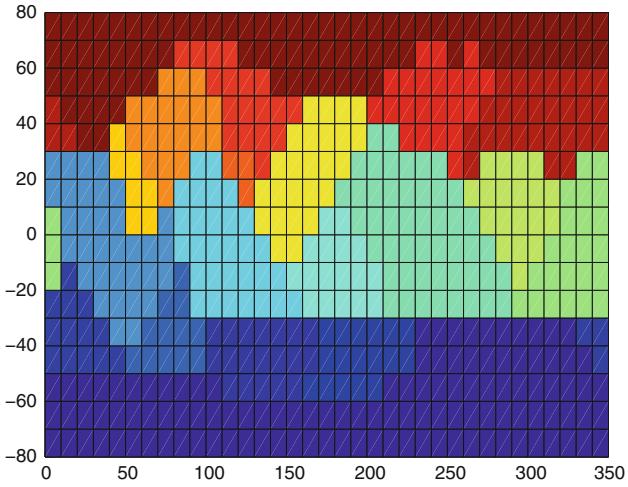

Fig. 4 Community structure for a spatio-temporal variability that is white with respect to time, and spatially correlated with a decorrelation length of 3,000 km on the sphere. This structure is not consistent with the community structures shown in Fig. 2. Thus, a null hypothesis that the observed structure in Fig. 2 can be reproduced using spatially correlated Gaussian white noise can safely be rejected

communities. Neither of these properties is consistent with what we observe for communities in the SAT, SLP, or 500 hPa height fields. In those observed fields, the number of communities is much smaller (about 5), and the structure of the communities is robust to adding or subtracting years from the analysis. Hence, it appears as if the observed community structure is not consistent with the structure arising from spatially correlated Gaussian white noise, and specifically, a null hypothesis that the observed structure can be reproduced using spatially correlated Gaussian white noise can safely be rejected.

4 Model results

Returning to Fig. 2, the right panels show the division into communities of networks constructed from model simulation of these three fields. The model used is the Geophysical Fluid Dynamics Laboratory (GFDL) CM2.1 coupled ocean/atmosphere model (GFDL CM2.1 development team 2006). The 1,860 pre-industrial conditions control run in the years 1950–2005 was used here. The resolution of these fields is also $10^0 \times 10^0$. For the simulated fields, the number of communities is 27, 16, and 249, respectively. However, as with the observations, many of these communities include very few points in the boundaries of what appears to be about five dominant communities. The modularity of the networks is 0.55, 0.49, and 0.80, respectively, indicating again large differences from random networks. We note here that because the number of communities is not necessarily the same in the model and in the observations, the color scheme used to show the spatial delineation of the communities is not the same in both observations and model simulations. This means that the same community may be represented by different colors in the observations and in the model. The reverse may also be possible: the same color may not represent the same community. What is relevant in comparing model simulations with observations in Fig. 2 is the spatial distribution and structure of the most highly populated communities regardless of their assigned color.

The observed general subdivision into the three latitudinal zones in the 500 hPa height and sea level pressure networks, as well as the north hemisphere-south hemisphere division in the surface temperature network is well captured by the model. However, the detailed structure of the communities, especially in the northern hemisphere, is not well captured by the model simulations. This indicates limitations in the models' ability to adequately describe certain dynamical aspects. For example, in the temperature network (bottom right panel) the model does not reproduce the temperature moderation over Europe due to the heat transport of the Gulf Stream. Rather, it produces an uniform variability over all land. This is consistent with insufficient resolution of oceanic sea surface temperatures and air–sea fluxes in the model. Similarly, in the 500 hPa height network (upper right panel) the model has difficulty reproducing the community structure associated with teleconnection patterns, indicating model deficiencies at simulating interannual atmospheric variability. In the sea level pressure network (middle right panel) it misses

the Rossby waves emanation from southern to northern hemisphere, marking model deficiencies in simulating the upper atmospheric flow over the tropical Pacific, a well-known problem in climate simulation (Hack et al. 1998). In spite of these structural differences, both model and observations agree that the number of communities is rather small.

This conclusion was verified by repeating the analysis using two additional different algorithms to divide the networks into communities. The first of these two approaches is based on finding the eigenvalues and eigenvectors of the modularity matrix (Newman 2006). The modularity matrix of the complete network is a real symmetric matrix B with elements

$$b_{ij} = a_{ij} - \frac{k_i k_j}{2M}$$

where a_{ij} are the elements of the adjacency matrix (equal to 1 if i and j are connected and zero otherwise), k_i is the number of connections of node i, and M is the total number of connections in the network. The method to split the network begins by estimating the eigenvalues and eigenvectors of the modularity matrix of the complete network. If all the elements in the eigenvector are of the same sign there is only one community. Otherwise, according to the sign of the elements of this vector, the network is divided into two parts (communities). Next, this process is repeated recursively for each community (using now the community modularity matrix), and so on. The other approach is based on a Bayesian approach to network modularity (Hofman and Wiggins 2008). The results from these two approaches (not shown) are not significantly different from those in Fig. 2. All methods delineate similar community structure with 4–5 effective communities. We note that due to spatial correlations, community structures do not change significantly when we consider the fields at a higher spatial resolution.

Our analysis brings up the more general question as to whether or not EOF analysis (which is based on variance explained) is indeed the appropriate method to study climate signals or oscillations. If variance is more important than how the system works (i.e. underlying topology), then EOF analysis may be a better approach. Otherwise, approaches like the network approach may be more appropriate. If there is an advantage of using networks is that the delineation of the major components is done "holistically" (meaning not in a set of EOFs) and it does not depend on the methodology and the assumptions used in estimating EOFs. The differences between the two methodologies may also account for possible mismatches in space between teleconnection patterns derived using network and EOF analysis.

5 Conclusions

It thus appears that the full complexity of the climate system is, over the time scales used here, suppressed into a small number of relevant communities. These communities involve major teleconnection patterns such as the PNA and NAO, communication between southern and northern hemisphere, storm tracks dynamics, and the barotropic and baroclinic property of lower and higher latitudes, respectively. This is consistent with recent results that demonstrated that synchronization of only a small number of slowly varying climate modes (associated with teleconnection patterns in the northern hemisphere and with ENSO) can explain all the decadal variability in the observed and modeled behavior of the climate system in the 20th century (Tsonis et al. 2007). According to recent results (Arenas et al. 2006) such synchronization is closely related to partitions of the network obtained by optimizing modularity and that this process unravels different topological scales in the network, which are relevant to underlying dynamics of the system. Our findings settle the issue of dimensionality of climate variability over decadal scales and support the view that over these scales climate collapses into distinct subsystems whose interplay dictates decadal variability, while at the same time provide clues as to what these subsystems might be. As such, while 'weather' may be complicated, 'climate' may be complex but not complicated. A direct consequence of our results is that a dynamical reconstruction directly from a small number of climate modes/subsystems may be attempted to extract differential equations that mimic something like the original data. Such an approach may provide an alternative and direct window to study low frequency variability in climate. Work in this area is in progress and will be reported later elsewhere.

Acknowledgments Kyle Swanson and Anastasios Tsonis are funded by NSF grant AGS-0902564. Geli Wang is funded by NSFC 40890052. Luciano da F. Costa thanks CNPq (301303/06-1) and FAPESP (05/00587-5) for sponsorship. Francisco Aparecido Rodriges is grateful to FAPESP (07/50633-9).

References

Albert R, Barabasi A-L (2002) Statistical mechanics of complex networks. Rev Mod Phys 74:1–54

Ambaum MHP, Hoskins BJ, Stephenson DB (2001) Arctic oscillation or North Atlantic oscillation? J Clim 14:3495–3507

Arenas A, Diaz-Guilera A, Perez-Vicente CJ (2006) Synchronization reveals topological scales in complex networks. Phys Rev Lett 96:114102

Barnston AG, Livezey RE (1987) Classification, seasonality, and persistence of low-frequency atmospheric circulation patterns. Mon Wea Rev 115:1083–1126

da F. Costa L, Rodrigues FA, Travieso G, Villas Boas PR (2007) Characterization of complex networks: a survey of measurements. Adv Phys 56:167–242

Eichler T, Higgins RW (2006) Climatology and ENSO-related variability of North American extratropical cyclone activity. J Clim 19:2076–2093

Elsner JB, Jagger TH, Fogarty EA (2009) Visibility network of United States hurricanes. Geophys Res Lett 36:L16702. doi:10.1029/2009GL039129

Farkas IJ, Jeong H, Vicsek T, Barabási A-L, Oltvai ZN (2003) The topology of the transcription regulatory network in the yeast *Saccharomyces cerevisiae*. Physica A 318:601–612

Favre A, Gershunov A (2006) Extra-tropical cyclonic/anticyclonic activity in North-Eastern Pacific and air temperature extremes in Western North America. Clim Dyn 26:617–629

Favre A, Gershunov A (2009) North Pacific cyclonic and anticyclonic transients in a global warming context: possible consequences for Western North American daily precipitation and temperature extremes. Clim Dyn 32:969–987

GFDL CM2.1 development team (2006) GFDL's CM2 global coupled models, parts 1–4. J Clim 19:643–740

Girvan M, Newman MEJ (2002) Community structure in social and biological networks. Proc Natl Acad Sci USA 99:7821–7826

Gozolchiani A, Yamasaki K, Gazit O, Havlin S (2008) Pattern of climate network blinking links follow El Nino events. Europhys Lett 83:28005

Guimera R, Amaral LAN (2005) Functional cartography of complex metabolic networks. Nature 433:895–900

Hack JJ, Kiehl JT, Hurrell JW (1998) The hydrologic and thermodynamic characteristics of NCAR CCM3. J Clim 11:1179–1206

Held IM, Ting M, Wang H (2002) Northern winter stationary waves: theory and modeling. J Clim 15:2125–2144

Hofman JM, Wiggins CH (2008) A Bayesian approach to network modularity. Phys Rev Lett 100:258701

Holme P, Huss M, Jeong H (2003) Subnetwork hierarchies of biochemical pathways. Bioinformatics 19:532–543

Kistler R et al (2001) The NCEP/NCAR 50-year reanalysis: monthly means, CD-ROM and documentation. Bull Am Meteorol Soc 82:247–267

Lorenz EN (1991) Dimension of weather and climate attractors. Nature 353:241–244

Mantegna RN (1999) Hierarchical structure in financial markets. Eur Phys J B 11:193–197

Mantua NJ, Hare SR, Zhang U, Wallace JM, Francis RC (1997) A Pacific interdecadal climate oscillation with impacts on salmon productions. Bull Am Meteor Soc 78:1069–1079

Newman MEJ (2006) Modularity and community structure in networks. Proc Natl Acad Sci USA 103:8577–8582

Newman MEJ, Girvan M (2004) Finding and evaluating community structure in networks. Phys Rev E 69:026113

Strogatz SH (2001) Exploring complex networks. Nature 410:268–276

Swanson KL, Tsonis AA (2009) Has the climate recently shifted? Geophys Res Lett 36:L06711. doi:10.1029/2008GL037022

Thompson DWJ, Wallace JM (1998) The Arctic Oscillation signature in the wintertime geopotential height and temperature fields. Geophys Res Lett 25:1297–1300

Tsonis AA (1992) Chaos: from theory to applications. Plenum, NY

Tsonis AA (2001) The impact of nonlinear dynamics in the atmospheric sciences. Int J Bifurcat Chaos 11:881–902

Tsonis AA, Elsner JB (1989) Chaos, strange attractors and weather. Bull Am Meteorol Soc 70:16–23

Tsonis AA, Elsner JB (1996) Mapping the channels of communication between the tropics and higher latitudes in the atmosphere. Physica D 92:237–244

Tsonis AA, Swanson KL (2008) Topology and predictability of El Nino and La Nina networks. Phys Rev Lett 100:228502

Tsonis AA, Swanson KL, Roebber PJ (2006) What do networks have to do with climate? Bull Am Meteorol Soc. doi:10.1175/BAMS-87-5-585

Tsonis AA, Swanson KL, Kravtsov S (2007) A new dynamical mechanism for major climate shifts. Geophys Res Lett 34:L13705. doi:10.1029/2007GL030288

Tsonis AA, Swanson KL, Wang G (2008) On the role of atmospheric teleconnection in climate. J Clim 21:2990–3001

Wallace JM, Gutzler DS (1981) Teleconnections in the geopotential height field during the northern hemisphere winter. Mon Wea Rev 109:784–812

Wang H, Fu R (2000) Influence of ENSO SST anomalies and water storm-tracks on the interannual variability of the upper tropospheric water vapor over the Northern Hemisphere extratropics. J Clim 13:59–73

Webster PJ, Holton JR (1982) Wave propagation through a zonally varying basic flow: the influences of mid-latitude forcing in the equatorial regions. J Atmos Sci 39:722–733

Yamasaki K, Gozolchiani A, Havlin S (2008) Climate networks around the globe are significantly affected by El Nino. Phys Rev Lett 100:228501